

# Spin-Polarized Electron Transport Processes at the Ferromagnet/Semiconductor Interface

J. A. C. Bland, Atsufumi Hirohata, Yong-Bing Xu, Christian M. Guertler, and Stuart N. Holmes

**Abstract**—Circularly polarized light was used to excite electrons with a spin polarization perpendicular to the film plane in ferromagnet/semiconductor hybrid structures. The Schottky characteristics at the interface were varied by using NiFe, Co and Fe as the ferromagnet. The Schottky characteristics were clearly observed with NiFe and Co/GaAs, while almost ohmic  $I - V$  characteristics were seen with Fe/GaAs. At negative bias a helicity-dependent photocurrent, dependent upon the magnetization configuration of the film and the Schottky barrier height, was detected upon modulating the polarization from right to left circular. For the magnetization along or perpendicular to the surface normal, the helicity-dependent photocurrent  $I^n$  or  $I^0$ , respectively, was measured. The asymmetry  $P = (I^n - I^0)/(I^n + I^0)$  of the helicity-dependent photocurrent decreases upon increasing the doping density of the GaAs substrates.  $P$  also decreases with photon energy  $h\nu$  as found for the polarization of photoexcited electrons in GaAs. In NiFe/GaAs samples for  $h\nu = 1.59$  eV,  $P = 16\%$  for  $n^+ = 10^{23}$  m $^{-3}$  and  $P = -23\%$  for  $p^- = 10^{25}$  m $^{-3}$  doped substrates, i.e.  $P$  is comparable in magnitude to the theoretically predicted spin polarization of 50% for the optically pumped conduction band in GaAs. The results provide unambiguous evidence of spin-polarized electron transport through the ferromagnet/semiconductor interface and show that the Schottky barrier height controls the spin-polarized electron current passing from the semiconductor to the ferromagnet. The asymmetry data indicates that spin-polarized electrons are transmitted from the semiconductor to the ferromagnet with a high efficiency.

**Index Terms**—Ferromagnet/semiconductor interface, photon helicity, Schottky barrier, spin-polarized electron.

## I. INTRODUCTION

THE POSSIBILITY of realizing a spin-dependent field effect transistor (spin FET) [1] remains an important goal in magnetoelectronics [2]. Since Datta and Das raised the possibilities for developing a spin FET [1], a great number of studies [3]–[6] on device structures based on ferromagnet (FM)/semiconductor (SC) hybrid systems have been carried out. A spin FET, for example, offers the prospect of fast operation and miniaturization [2]. Johnson described spin-dependent electron transport in a Au film-based transistor [3]. In such a device, the operation depends on both the injection of a spin-polarized current into the SC [4], [5] and the “spin filter” effects in the FM [6]. Attempts to inject a spin-polarized

electron current to a SC using a FM metal indicate that such polarized current may be very small [5], [7], [8]. On the other hand, significant spin injection from a ferromagnetic SC to a nonmagnetic SC has been claimed at low temperature [9]–[11].

One way of achieving spin injection is based on spin-dependent tunneling through metal/oxide insulator/semiconductor (MOS) junctions. The possibility of passing a spin-dependent current through thin film tunnel junctions of both Co/Al<sub>2</sub>O<sub>3</sub>/GaAs and Co/ $\tau$ -MnAl/AlAs/GaAs using photoexcited spin-polarized electron has been discussed by Prins *et al.* [12]. For the former structure, a spin-dependent tunneling current was reported, while only magneto-optical effects were seen in the latter structure. A great many studies of spin-dependent tunneling through MOS junctions have since been reported. As these measurements have been performed using back illumination of the circularly polarized light, optically excited electrons in the SC can be used to realize spin-polarized scanning tunneling microscopy (SP-STM) using sharp SC tips as theoretically proposed [14], [32]. Some recent experiments suggest that such SP-STM may provide magnetic information [15], [33].

However, due to the presence of the oxide interface, the spin-polarized tunneling through the MOS junction mechanism is very sensitive to interface properties. For the direct FM/SC interface, a Schottky barrier is formed which also gives rise to tunneling under appropriate bias conditions with highly doped SC. In such a system, circularly polarized light can excite spin-polarized electrons mainly in the SC. Due to the spin polarization at the Fermi level in the metal, the FM layer can be expected to act as a “spin filter” for polarized electrons transported through the interface. Alvarado *et al.* have observed spin-polarized electron transport at the FM/SC interface using electroluminescence (EL) [16]. However, it is still not clear whether spin-polarized tunneling at the direct FM/SC interface occurs through the Schottky barrier (in either direction). Evidence of spin-polarized current effects associated with photoexcited electron transport at Schottky diode interfaces based on NiFe/GaAs and Co/GaAs structures has been demonstrated recently [17]–[19]. However, these effects are seen at forward bias and do not correspond to tunneling from the SC to the FM [17], [18]. In such experiments, the advantage of photoexcitation is that the electron polarization in the SC can be controlled via the light polarization. A polarized electron current from the SC to the FM can therefore be included under appropriate bias conditions to test spin-polarized electron transport at the FM/SC interface. In addition, the effect of spin injection from the FM to the SC can be expected to add to or subtract from the total spin-polarized electron current.

Manuscript received February 14, 2000. This work was supported in part by EPSRC and EU (ESPRIT). The work of A. Hirohata was supported by Toshiba Europe Research Limited and Cambridge Overseas Trust.

The authors are with the Cavendish Laboratory, University of Cambridge, Cambridge CB3 0HE, England (e-mail: {jacob1; ah242; s.holmes}@phy.cam.ac.uk).

Publisher Item Identifier S 0018-9464(00)08317-5.

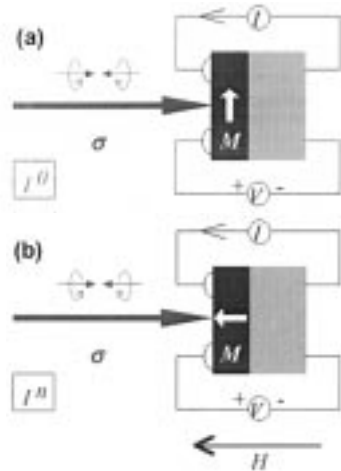


Fig. 1. Schematic configuration of the photoexcitation experiment. The laser ( $\lambda = 515, 633$  and  $780$  nm, and power  $30, 5$  and  $3$  mW, respectively) is polarized in the  $45^\circ$  direction. Right/left circular light is produced using a PEM. The bias dependent photocurrent is determined by  $I - V$  measurement methods combined with a lock-in technique. A schematic view of the FM/GaAs hybrid structure ( $3 \text{ mm} \times 3 \text{ mm}$ ) is also shown in this diagram. Two Al contacts on the surface ( $0.5 \text{ mm} \times 0.5 \text{ mm} \times 550 \text{ nm}$ ) and an ohmic contact on the bottom are used for the measurement. The value of the variable resistance for the measurement was chosen to be approximately the same as that of the resistance between the FM and the GaAs substrate. The magnetization  $M$  in the FM and the photon helicity  $\sigma$  are shown with the field applied normal to the sample. Experimental configurations, (a) without ( $I^0$ ) and (b) with ( $I^n$ ) a magnetic field, are also shown in the inset.

Here we present results which clarify the dependence of spin-polarized transport on the Schottky barrier height. We fabricated  $5 \text{ nm}$  thick ferromagnetic layers ( $\text{Ni}_{80}\text{Fe}_{20}$ , Co and Fe) directly onto GaAs substrates in an ultrahigh vacuum (UHV) chamber. Conventional  $I - V$  measurements were performed both with and without photoexcitation. A circularly polarized laser beam was then used together with an external magnetic field to investigate the spin-dependence of the photocurrent at the FM/GaAs interface at room temperature. By varying the Schottky barrier according to either the various FM materials or the doping density in the SC, the roles of photoexcitation in the SC and the FM are investigated. The photon energy dependence of the spin-dependent photocurrent is also studied and compared with that measured by photoemission experiments. For the FM, permalloy was chosen due to a large polarization difference at its Fermi level [20] and a small magneto-optical background [due to magnetic circular dichroism (MCD)], and compared with Co and Fe samples. Since the epitaxial growth of the FM transition metals on GaAs substrates has been well established [21], GaAs substrates were chosen for the present study [22].

## II. EXPERIMENTAL PROCEDURE

Fig. 1 shows a schematic diagram of the photoexcitation set-up with front illumination at room temperature. Conventional  $I - V$  measurements were made to investigate the Schottky characteristics of the samples. Laser light ( $515 \leq \lambda \leq 780 \text{ nm}$ ) perpendicular to the sample surface was used and the bias dependence of the current through the FM/GaAs interface ( $-2.5 < V < 1.5 \text{ V}$ ) was measured with and without optical excitation. The polarization of the beam was then modulated from right to left circular using a

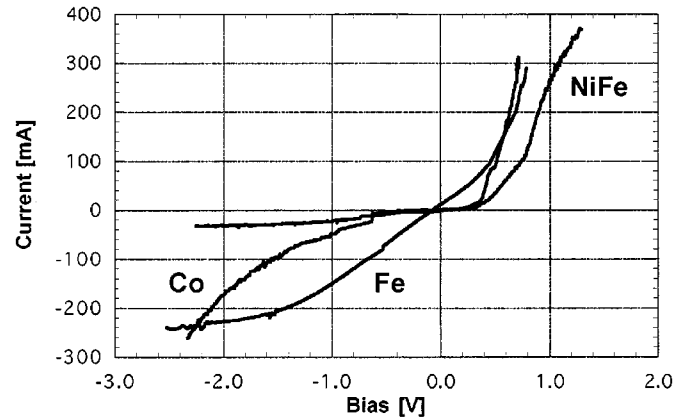


Fig. 2. Bias dependence of the current through the FM/GaAs (100) interface without photoexcitation ( $I - V$  curve) for the case of  $\text{Ni}_{80}\text{Fe}_{20}/\text{GaAs}$  ( $n^+ = 10^{23} \text{ m}^{-3}$ ), Co/GaAs ( $n^+ = 10^{24} \text{ m}^{-3}$ ) and (c) Fe/GaAs ( $n^+ = 10^{23} \text{ m}^{-3}$ ).

photo-elastic modulator (PEM) with 100% circular polarization at a frequency of  $50 \text{ kHz}$ . For the polarized illumination mode, the bias dependence of the ac helicity-dependent photocurrent  $I$  through the interface was probed both (a) in the remanent state ( $I^0$ ) and (b) under the application of a magnetic field ( $H = 1.8 \text{ T}$ ) sufficient to saturate the magnetization along the plane normal ( $I^n$ ). In the case of  $I^0$ , the photon helicity  $\sigma$  is perpendicular to the magnetization of the FM ( $\sigma \perp M$ ), while the helicity is either parallel or anti-parallel to the magnetization ( $\sigma // M$ ) for  $I^n$ .  $I^0$  and  $I^n$  are a measure of the difference in photocurrent for right/left circular polarization for the in-plane and perpendicular magnetization configurations, respectively.

We produced samples of  $3 \text{ nm Au}/5 \text{ nm FM}/\text{GaAs}$  (100) and (110) ( $n^+ = 10^{23}, 10^{24}$  and  $p^- = 10^{25} \text{ m}^{-3}$  doped) using molecular beam epitaxy (MBE) techniques in UHV. The ohmic contacts on the bottom of the  $n$ - and  $p$ -type substrates were prepared by evaporating  $100 \text{ nm}$  thick GeAuNi and AuBe, respectively, and then annealed at  $770 \text{ K}$  for two minutes. The GaAs substrates were cleaned for two minutes using an oxygen plasma and loaded into the UHV chamber. The FM films were epitaxially grown at a rate of approximately one monolayer per minute by e-beam evaporation. The substrate temperature was held at  $300 \text{ K}$  and the pressure was around  $7 \times 10^{-10} \text{ mbar}$  during the growth. The deposition rate was monitored by a quartz microbalance which was calibrated using RHEED oscillations of Fe on a Ag (100) single crystal substrate. After the growth, the FM films were covered by a Au capping layer. Two Al electrical contacts were evaporated onto the Au layer. A computer controlled bias voltage was applied between one Al contact and the bottom ohmic contact and the current through another Al contact and the substrate was measured using a lock-in technique. As the polarized laser beam enters from the Au capping layer side, these structures provide a way of avoiding laser absorption at the bottom surface of the SC, as occurs under back illumination [23].

## III. RESULTS AND DISCUSSION

### A. $I - V$ Characteristics with Various Ferromagnets

Fig. 2 shows the  $I - V$  curves of the FM/GaAs (100) samples without photoexcitation measured by the four-terminal method.

The Schottky barrier ( $\phi_b$ ) of these samples varies as the barrier defines the shape of the  $I - V$  curves via the Schottky equation

$$J = A^{**} T^2 \exp(-q\phi_b/kT) \exp\{(qV/kT) - 1\}.$$

The value of the ideality factor [23] was found to be 6.7 and 2.9 for NiFe and Co, respectively, while in the case of Fe, the  $I - V$  characteristic is almost ohmic. It should be noted that the  $I - V$  curves of both NiFe and Co samples also contain ohmic linear components and this makes it difficult to estimate the Schottky barrier height.

Representative  $I - V$  curves, corresponding to the bias dependence of the photocurrent, was also measured for these samples with unpolarized photoexcitation. The same set-up as that of the  $I - V$  measurement was used but with laser illumination. Intensity modulation of the laser beam at 105 Hz was used to create a reference signal for the lock-in amplifier to separate the photocurrent contribution to the total current. The entire  $I - V$  curves except that of the Fe sample are shifted to negative current values as expected for conventional Schottky diodes [24].

The Schottky barrier height  $\phi_b$  has been reported to be 0.66–0.70 eV for both Ni and Fe [25], which is approximately the same as the bias voltage at which the NiFe diode is turned on. With Co as the FM, the device is turned on at a bias of 0.4 V. The Schottky barrier height for Co/GaAs has been reported to be 0.42–0.66 eV [25] in agreement with our observation. With Fe, however, no photocurrent is detected at zero bias, which may be consistent with both the existence of an intermixed interfacial layer and an absence of midgap states [26]. The resistance of the Fe/GaAs system with photoexcitation is higher than that without photoexcitation.

Difference between the  $I - V$  characteristics of the samples are expected, since the electronic structure differs. In the case of NiFe, since the density of states can be assumed to be almost the same as that of Ni [27], [28], the density of states is at its maximum at the Fermi surface and sharply decreases away from the Fermi level [28]. With Co, the density of states at the Fermi energy exhibits a broad maximum within  $\pm 0.5$  eV from the Fermi energy [29]. It is therefore easy to detect the photocurrent from these two systems. In Fe, however, since the density of states is neither large nor sharp around the Fermi level [27], the photocurrent should be extremely small.

### B. Helicity-Dependent Photocurrent with Various FM

The helicity-dependent photocurrent observed using a He–Ne laser ( $\lambda = 633$  nm) is shown in Fig. 3 with ( $I^n$ ) and without ( $I^0$ ) perpendicular saturation. In the case of NiFe/GaAs (100) ( $n^+ = 10^{23} \text{ m}^{-3}$ ) [see Fig. 3(a)], for instance, it should be noted that the observed helicity-dependent photocurrent values for  $I^n$  and  $I^0$  satisfy  $I^n < I^0$  as previously reported [17]. Both  $I^n$  and  $I^0$  possess an offset due to the photocurrent across the interface discussed above. The bias dependence of the helicity-dependent photocurrent difference  $\Delta I (=I^n - I^0)$  of  $\sim -15$  nA is almost constant in the bias range of  $V < 0.7$  V. The negative values of both  $I^0$  and  $I^n$  mean that electron current mainly flows from the FM to the SC. The valence band electrons in the SC are excited into the conduction band by the circularly polarized light and tunnel through the Schottky barrier into the FM as shown

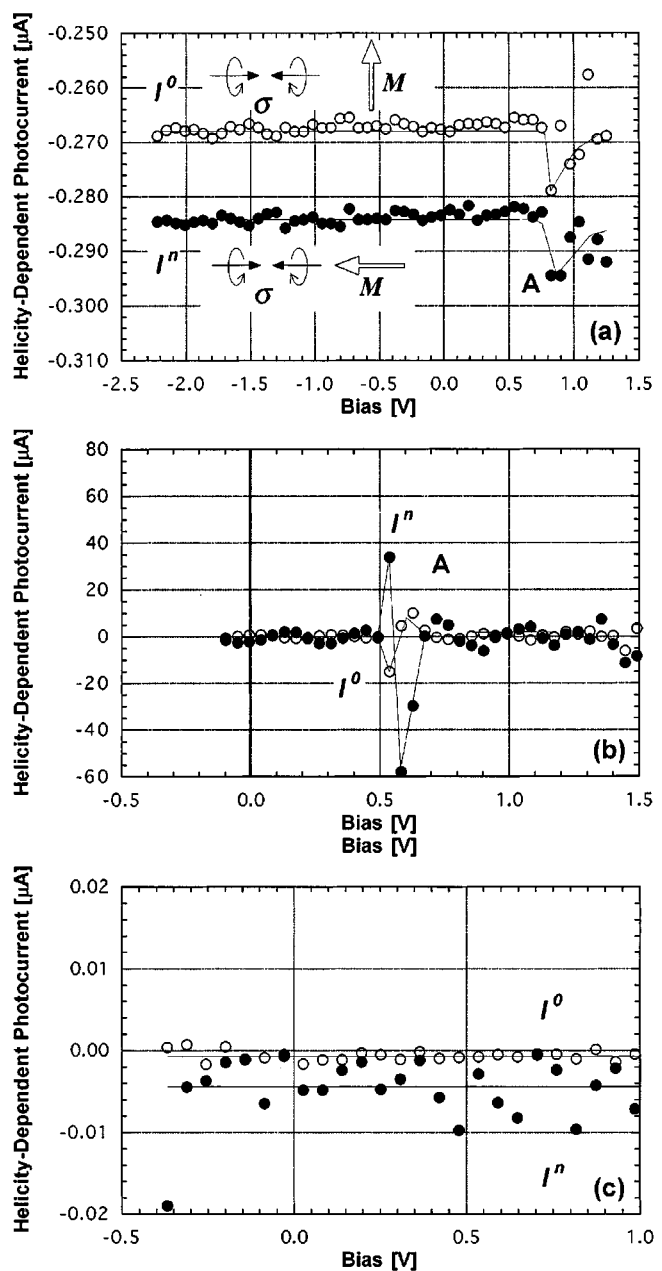


Fig. 3. Bias dependence of the helicity-dependent photocurrent without (solid line with open circles,  $I^0$ ) and with the applied magnetic field (solid line with closed circles,  $I^n$ ) in the case of (a) Ni<sub>80</sub>Fe<sub>20</sub>/GaAs (100) ( $n^+ = 10^{23} \text{ m}^{-3}$ ), (b) Co/GaAs (100) ( $n^+ = 10^{24} \text{ m}^{-3}$ ) and (c) Fe/GaAs (100) ( $n^+ = 10^{23} \text{ m}^{-3}$ ). The magnetization  $M$  in the FM and the photon helicity  $\sigma$  are also shown without and with the field application.

schematically in Fig. 4(a). In the remanent state [see left hand side of Fig. 4(a)], since the magnetization in the FM is orthogonal to the photoexcited spin polarization, both up and down spin electrons in the SC can flow into the FM, which opposes the electron current from the FM. At perpendicular saturation [see right hand side in Fig. 4(a)], on the other hand, the up spin electron current from the SC is filtered due to the spin split density of states at the Fermi level of the FM. This means that more net current flows into the SC at perpendicular saturation than that in the remanent state, as observed resulting in  $I^n < I^0$ . The observation that  $I^n < I^0$  provides clear evidence that spin-polarized

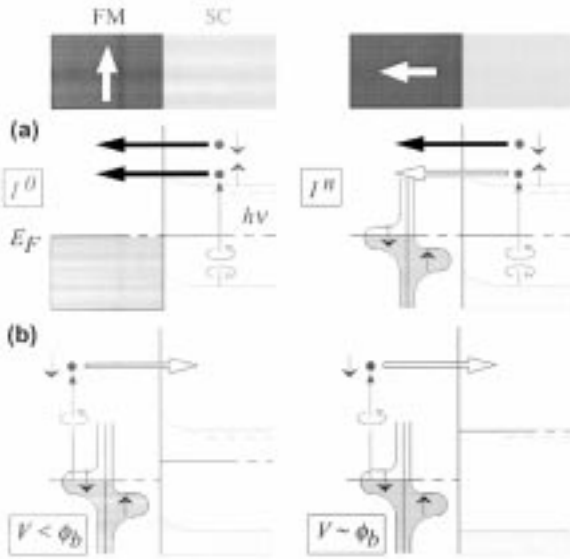


Fig. 4. Schematic diagrams illustrating (a) the “spin filter” and (b) the spin injection mechanism for photoexcited electron transport at the FM/SC interface.

transport from the SC to the FM occurs under the application of a perpendicular magnetic field (“spin filter” effects).

In Fig. 3(a), the bias dependence of the helicity-dependent photocurrent is shown. Since electrons are also excited in the permalloy layer by both the bias and the photon energy, inelastically scatter and then propagate over the barrier [23], the negative peak A is more likely to be related to spin-polarized transport from the FM to the SC as shown in Fig. 4(b) (spin injection). At  $V \sim \phi_b$ , the conduction band in the SC flattens and electrons can easily enter the SC from the FM. The Schottky barrier height  $\phi_b$  has been reported to be 0.66–0.70 eV for Ni and Fe [25], which is approximately the same as the bias voltage for peak A.

With  $n^+ = 10^{24} \text{ m}^{-3}$ , a similar tendency can be seen [19], although peak A for  $I^n$  is much broader than that of  $I^0$ . In reverse bias, a constant difference between  $I^0$  and  $I^n$  is again observed ( $\sim 0.06 \mu\text{A}$ ). In the case of  $p^- = 10^{25} \text{ m}^{-3}$ , the difference  $\Delta I$  is observed to be less than 3 nA and to satisfy  $I^n > I^0$ , suggesting that these features are related to the height of the Schottky barrier at the interface. Both  $I^0$  and  $I^n$  are again constant in reverse bias but of almost the same magnitude, which means that there is no significant spin-polarized current through the interface.

Fig. 3(b) shows the helicity-dependent photocurrent observed with Co/GaAs (100) ( $n^+ = 10^{24} \text{ m}^{-3}$ ).  $I^0$  is almost constant ( $\sim 99 \text{ nA}$ ), while  $I^n$  fluctuates by approximately  $-1.13 \pm 0.31 \mu\text{A}$ . The difference  $\Delta I$  is almost zero for much of the bias range, except close to peak A. This provides a clear check on possible experimental asymmetries.

Similarly to the NiFe samples, peak A is also seen (at  $V \sim 0.6 \text{ V}$ ) as previously reported [18]. It should be noted that these values of the bias voltage correspond to a broad maximum of the spin polarization in Co as discussed above [29]. The peak is again probably related to spin-polarized current (spin injection) from the FM to the SC as discussed above. It should be noted that spin injection effects are larger than spin filter effects in Co/GaAs, which suggests that Co may be an appropriate choice

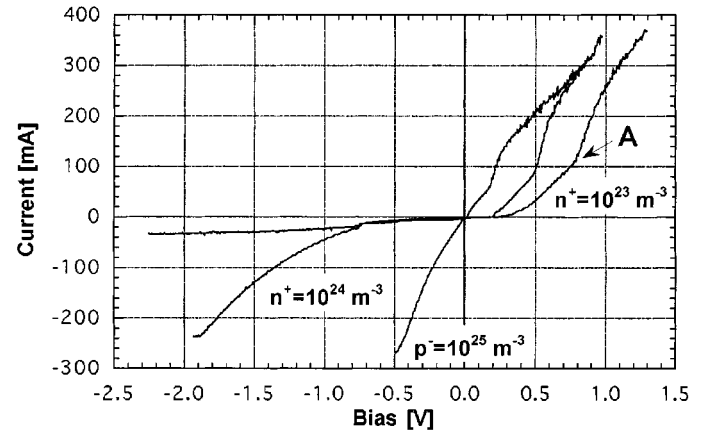


Fig. 5. Bias dependence of current through the  $\text{Ni}_{80}\text{Fe}_{20}/\text{GaAs}$  (100) ( $n^+ = 10^{23}, 10^{24}$  and  $p^- = 10^{25} \text{ m}^{-3}$ ) interface obtained without photoexcitation ( $I - V$  curve).

of material for spin injection devices as already used [12]. With  $p^- = 10^{25} \text{ m}^{-3}$ ,  $\Delta I \sim 35 \text{ nA}$ , which corresponds to a decrease with increasing doping density as observed with NiFe/GaAs. The position of peak A shifts to  $V \sim 0.1 \text{ V}$ , which is similar to that seen with the NiFe/GaAs samples.

Fig. 3(c) shows the Fe/GaAs (100) ( $n^+ = 10^{23} \text{ m}^{-3}$ ) results.  $I^0$  is almost constant ( $-0.92 \text{ nA}$ ), while  $I^n$  is approximately  $-4.3 \text{ nA}$ .  $\Delta I$  is calculated to be about  $-3.4 \text{ nA}$ . No particular peak is seen, which is consistent with the ohmic characteristics of the Fe/GaAs samples. This also provides a check on possible experimental asymmetries.

### C. Polarization with Variable Doping Density

Since permalloy samples show both a large photocurrent at zero bias and good Schottky characteristics, we focus on the dependence of the spin-polarized electron transport on the Schottky barrier height using NiFe/GaAs samples.

Fig. 5 shows the  $I - V$  curves of the  $\text{Ni}_{80}\text{Fe}_{20}/\text{GaAs}$  (100) samples without photon excitation measured by the four-terminal method. It should be noted that every  $I - V$  curve possesses a small feature (A) in forward bias around the Schottky barrier height  $\phi_b$ . The ideality factor [23] was calculated to be 6.7, 5.4 and 4.0 for  $n^+ = 10^{23}, 10^{24}$  and  $p^- = 10^{25} \text{ m}^{-3}$ , respectively. These samples also contain ohmic linear components in the  $I - V$  curves. By varying the doping density, the Schottky barrier height is changed in the NiFe/GaAs hybrid structures.

The asymmetry of the spin-polarized current through the NiFe/GaAs interface  $P = (I^n - I^0)/(I^n + I^0)$  induced by He-Ne laser light is shown in Fig. 6 for three different values of the GaAs doping density. With  $n^+ = 10^{24} \text{ m}^{-3}$ , for example, almost constant asymmetry ( $P \sim 4.5\%$ ) can be seen in the bias range of  $-1.5 < V < 0.3 \text{ V}$ , which is likely to be related to the spin-polarized photocurrent propagating from the SC to the FM as discussed above. For  $n^+ = 10^{23} \text{ m}^{-3}$ , the corresponding value is  $P \sim 3\%$ , while for  $p^- = 10^{25} \text{ m}^{-3}$ ,  $P \sim 0$ . It should be noted that these values of  $P$  depend on the resistivity across the FM/SC interface. The total resistance is 60, 200 and  $15 \Omega$  for the  $n^+ = 10^{23}, 10^{24}$  and  $p^- = 10^{25} \text{ m}^{-3}$  doped substrates, respectively. We conclude from the above results

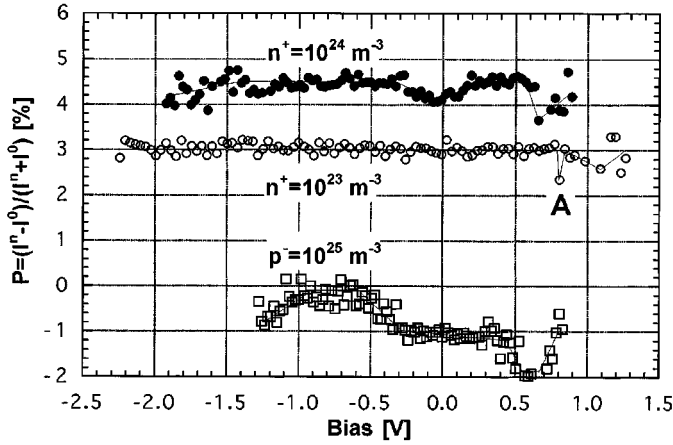


Fig. 6. Bias dependence of asymmetry  $P = (I^n - I^0)/(I^n + I^0)$  with  $\text{Ni}_{80}\text{Fe}_{20}/\text{GaAs}$  (100) ( $n^+ = 10^{23}$ ,  $10^{24}$  and  $p^- = 10^{25} \text{ m}^{-3}$ ).

that the magnitude of the spin-polarized current in reverse bias scales with the Schottky barrier height, as is expected for spin-polarized tunneling across the barrier. This asymmetry is much larger than the estimated value (0.2%) caused by MCD [17] and MCD effects can therefore be excluded.

A small peak A for  $n^+ = 10^{23} \text{ m}^{-3}$  ( $V \sim 0.8 \text{ V}$ ) at the Schottky barrier height  $\phi_b$  is again seen in this figure, although the feature is small. The position of the feature is almost the same as that of peak A in Fig. 3(a), which again supports the view that the spin-polarized current (spin injection) from the FM to the SC is enhanced at  $V \sim \phi_b$ . At peak A,  $P$  is estimated to be 2.5%, which is much larger than was previously observed in similar samples (0.5%) [17]. Peak A is also seen with  $n^+ = 10^{24} \text{ m}^{-3}$  around 0.7 V, which is almost at the same value of bias voltage at which peak A is observed in the helicity-dependent photocurrent [19]. With  $p^- = 10^{25} \text{ m}^{-3}$ , peak A is seen at  $V \sim 0.6 \text{ V}$ . As peak A shifts toward 0 V with increasing doping density, we conclude this peak shift is due to the lowering of the Schottky barrier height  $\phi_b$  with doping. Peak A also becomes broader with doping density.

In the case of Co/GaAs, the asymmetry decreases with increasing doping density as observed with the NiFe samples. The difference in the helicity-dependent photocurrent is also almost constant and is different from that observed with the Co/Al<sub>2</sub>O<sub>3</sub>/GaAs system, in which  $\Delta I/I \sim \text{few \%}$  at reverse bias, diverges gradually at zero bias and does not show any peak at forward bias [13]. Since MCD in Co has been reported to be  $\sim 0.15\%$  [13], the MCD effects on the helicity-dependent photocurrent measurements can again be excluded. For the Fe/GaAs structures, the asymmetry is again difficult to estimate but is found to decrease with doping density.

These observations suggest that the spin-polarized photocurrent from the SC to the FM is suppressed by electron transport (spin injection) from the FM to the SC under the application of a forward bias  $V \sim \phi_b$ .

#### D. Asymmetry with Variable Photon Energy

The photon energy dependence of the current asymmetry  $P$  was also measured. The absolute value of  $P$  increases with

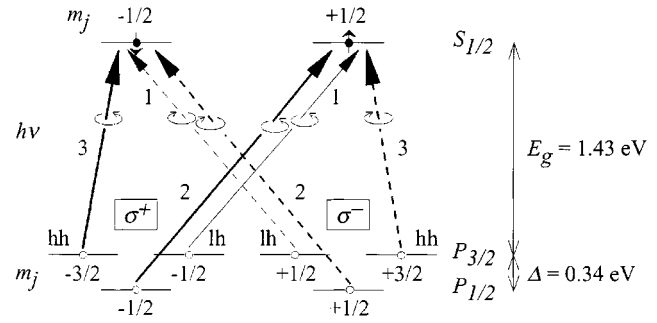


Fig. 7. Schematic diagram of the allowed transitions for right ( $\sigma^+$ , solid lines) and left ( $\sigma^-$ , dashed lines) circularly polarized light with GaAs at room temperature. The selection rule is  $\Delta m_j = +1$  for  $\sigma^+$  and  $\Delta m_j = -1$  for  $\sigma^-$ . The numbers near the arrows represent the relative transition probabilities. The magnetic quantum numbers are also indicated at the energy levels. The heavy and light holes are abbreviated to hh and lh, respectively.

decreasing photon energy from almost zero ( $h\nu = 2.41 \text{ eV}$ ) up to 20% ( $h\nu = 1.59 \text{ eV}$ ), which corresponds closely to the reported photon energy dependence of the photoelectron spin polarization in GaAs [30].

In GaAs, the valence band maximum and the conduction band minimum is at  $\Gamma$  with an energy gap  $E_g = 1.43 \text{ eV}$  at room temperature, indicating that the only transitions induced by the photon energy  $h\nu$  occurs at  $\Gamma$  (direct gap semiconductor) [30], [31]. The valence band ( $p$ -symmetry) splits into four-fold degenerate  $P_{3/2}$  and two-fold degenerate  $P_{1/2}$  states, which lie  $\Delta = 0.34 \text{ eV}$  below  $P_{3/2}$  at  $\Gamma$ , whereas the conduction band ( $s$ -symmetry) is two-fold degenerate  $S_{1/2}$  as schematically shown in Fig. 7. When  $h\nu = E_g$ , circularly polarized light excites electrons from  $P_{3/2}$  to  $S_{1/2}$ . According to the selection rule ( $\Delta m_j = \pm 1$ ), the two transitions for each photon helicity ( $\sigma^+$  and  $\sigma^-$ ) are possible, however the relative transition probabilities for light and heavy holes need to be taken into account in order to estimate the net spin polarization [30]. Although the maximum polarization is expected to be 50% in theory, the maximum is experimentally observed to be  $\sim 40\%$  at the threshold [10], [30]. Since the polarization also depends on the thickness of the overlayers [10], our results for the estimated asymmetry  $P$  between 16–23% with  $10^{23}$  and  $10^{25}$  doped substrates, respectively, are in a good agreement with these reported values. For  $E_g + \Delta < h\nu$ , the polarization decreases due to the mixture of light and heavy hole states with the split-off valence band states, which have an opposite sign [30].

These spin-polarized photoexcited electrons flow into the FM as described in Fig. 4. In the remanent state, both up and down spin electrons can pass across the Schottky barrier. At perpendicular saturation, on the other hand, since spin polarization occurs at the Fermi level, the up spin electrons are unable to penetrate the FM as described in Section III-B. Since the magnitude of the spin polarization at the Fermi level is  $\text{Fe} < \text{Co} < \text{NiFe}$  [27]–[29], the NiFe/GaAs structures possess the most efficient spin filtering effect for the photoexcited electrons from GaAs. This corresponds to the observed asymmetry  $P$  of almost the same magnitude as the maximum spin polarization in GaAs.

The observed photon energy dependence of  $P$  therefore supports our interpretation that spin-polarized electron transport

from the SC to the FM occurs at room temperature with high efficiency.

#### IV. CONCLUSION

We have observed a clear difference in the helicity-dependent photocurrent through the FM/GaAs interface according to the orientation of the sample magnetization with respect to the helicity at room temperature. An almost constant difference between the helicity-dependent photocurrent for perpendicular and parallel configurations is observed in reverse bias especially for NiFe/GaAs ( $n^+ = 10^{23}$  and  $10^{24} \text{ m}^{-3}$ ). This difference in photocurrent corresponds to a measure of the spin-polarized photocurrent tunneling from the SC to the FM associated with spin filter effects. In forward bias at an applied bias voltage approximately equal to the Schottky barrier height, a minor change in the bias dependence of the helicity-dependent photocurrent was observed, suggesting the existence of polarized electron transport (spin injection) from the FM to the SC. The estimated excitation energy dependent of the helicity-dependent photocurrent asymmetry was found to be in agreement with that of the reported photoelectron spin polarization.

#### ACKNOWLEDGMENT

The authors would like to thank Prof. G. Cheng for assistance with the Ar laser operation.

#### REFERENCES

- [1] S. Datta and B. Das, *Appl. Phys. Lett.*, vol. 56, pp. 665–667, February 1990.
- [2] G. A. Prinz, *Science*, vol. 282, pp. 1660–1663, November 1998.
- [3] M. Johnson, *J. Appl. Phys.*, vol. 75, pp. 6714–6719, May 1994.
- [4] A. Fert and S. F. Lee, *J. Magn. Magn. Mat.*, vol. 165, pp. 115–120, 1997.
- [5] P. R. Hammar, B. R. Bennet, M. J. Yang, and M. Johnson, *Phys. Rev. Lett.*, vol. 83, pp. 203–206, July 1999.
- [6] S. K. Upadhyay, R. N. Louie, and R. A. Buhrman, *Appl. Phys. Lett.*, vol. 74, pp. 3881–3883, June 1999.
- [7] F. G. Monzon, M. Johnson, and M. L. Roukes, *Appl. Phys. Lett.*, vol. 71, pp. 3087–3089, Nov. 1997.
- [8] S. Gardelis, C. G. Smith, C. H. W. Barnes, E. H. Linfield, and D. A. Ritchie, *Phys. Rev. B*, vol. 60, pp. 7764–7767, Sept. 1999.
- [9] M. Oestreich, J. Hübner, D. Hägele, P. J. Klar, W. Heimbrodt, W. W. Rühle, D. E. Ashenford, and B. Lunn, *Appl. Phys. Lett.*, vol. 74, pp. 1251–1253, Mar. 1999.
- [10] R. Fiederling, M. Keim, G. Reuscher, W. Ossau, G. Schmidt, A. Waag, and L. W. Molenkamp, *Nature*, vol. 402, pp. 787–790, Dec. 1999.
- [11] Y. Ohno, D. K. Young, B. Beschoten, F. Matsukura, H. Ohno, and D. D. Awschalom, *Nature*, vol. 402, pp. 790–792, Dec. 1999.
- [12] M. W. J. Prins, H. van Kempen, H. van Leuken, R. A. de Groot, W. van Roy, and J. de Boeck, *J. Phys.: Cond. Matt.*, vol. 7, pp. 9447–9464, 1995.
- [13] K. Nakajima, S. N. Okuno, and K. Inomata, *Jpn. J. Appl. Phys.*, vol. 37, pp. L919–L922, Aug. 1998.
- [14] S. N. Molotkov, *Surf. Sci.*, vol. 287/288, pp. 1098–1101, 1993.
- [15] K. Sueoka, K. Mukasa, and K. Hayakawa, *Jpn. J. Appl. Phys.*, vol. 32, pp. 2989–2993, June 1993.
- [16] S. F. Alvarado and P. Renaud, *Phys. Rev. Lett.*, vol. 68, pp. 1387–1390, Mar. 1992.
- [17] A. Hirohata, Y. B. Xu, C. M. Guertler, and J. A. C. Bland, *J. Appl. Phys.*, vol. 85, pp. 5804–5806, Apr. 1999.
- [18] ———, *IEEE Trans. Magn.*, vol. 35, pp. 2910–2912, Sept. 1999.
- [19] ———, *J. Appl. Phys.*, vol. 87, pp. 4670–4672, Apr. 2000.
- [20] S. Chikazumi, *Physics of Magnetism*. Oxford: Clarendon, 1997, pp. 163–196.
- [21] Y. B. Xu, E. T. M. Kernohan, D. J. Freeland, A. Ercole, M. Tselepi, and J. A. C. Bland, *Phys. Rev. B*, vol. 58, pp. 890–896, July 1998.
- [22] J. M. Kikkawa and D. D. Awschalom, *Phys. Rev. Lett.*, vol. 80, pp. 4313–4316, May 1998.
- [23] S. M. Sze, *Physics of Semiconductor Devices*. New York: Wiley, 1981, pp. 245–311.
- [24] R. H. Bube, *Photoelectronic Properties of Semiconductors*. Cambridge: Cambridge University Press, 1992, pp. 244–279.
- [25] L. Magaud and F. Cyrot-Lackmann, *Encyclopedia of Applied Physics*. New York: VCH, 1996, vol. 16, pp. 573–591.
- [26] B. T. Jonker, O. J. Glembocki, R. T. Holm, and R. J. Wagner, *Phys. Rev. Lett.*, vol. 79, pp. 4886–4889, Dec. 1997.
- [27] I. I. Mazin, *Phys. Rev. Lett.*, vol. 83, pp. 1427–1430, Aug. 1999.
- [28] B. Nadgorny, R. J. Soulen Jr., M. S. Osofsky, I. I. Mazin, G. Laprade, R. J. M. van de Veerdonk, A. A. Smits, S. F. Cheng, E. F. Skelton, and S. B. Qadri, *Phys. Rev. B*, vol. 61, pp. R3788–R3791, Feb. 2000.
- [29] C. Li, A. J. Freeman, and C. L. Fu, *J. Magn. Magn. Mater.*, vol. 75, pp. 53–60, 1988.
- [30] D. T. Pierce and F. Meier, *Phys. Rev. B*, vol. 13, pp. 5484–5500, June 1976.
- [31] S. Adachi, *GaAs and Related Materials*. Singapore: World Scientific, 1994, p. 145.
- [32] R. Laiho and H. J. Reittu, *ibid.*, vol. 289, pp. 363–369, 1993.
- [33] Y. Suzuki, W. Nabhan, and K. Tanaka, *Appl. Phys. Lett.*, vol. 71, pp. 3153–3155, Nov. 1997.